Supplement of Atmos. Chem. Phys., 21, 10015–10037, 2021
https://doi.org/10.5194/acp-21-10015-2021-supplement

Supplement of

Anthropogenic and natural controls on atmospheric δ^{13}C-CO_2 variations in the Yangtze River delta: insights from a carbon isotope modeling framework

Cheng Hu et al.

Correspondence to: Cheng Hu (nihaohucheng@163.com, huxxx991@umn.edu) and Timothy J. Griffis (timgriffis@umn.edu)

This document includes 2 tables and 4 figures:

Method to derive $\boldsymbol{\delta}^{13}$C-CO_2 background

$$\delta_a^{13} \times C_a = \delta_s \times (C_a - C_b) + \delta_b \times C_b$$

The $\boldsymbol{\delta}_b$ background can be calculated based on above equation, here only C_b is not observed and with low bias as assessed before, $\boldsymbol{\delta}_s$ is the mixture of end-members by regional sources and it can be derived by independent Miller-Tans and keeling plots regressions approaches at monthly intervals, the nighttime (22:00-08:00) $\boldsymbol{\delta}$s will be used for these 2 approaches, see details of $\boldsymbol{\delta}_s$ calculations in Xu et al. (2017). C_a and $\boldsymbol{\delta}_a^{13}$ are observed atmospheric CO_2 mixing ratio and $^{13}C/^{12}C$ ratio.

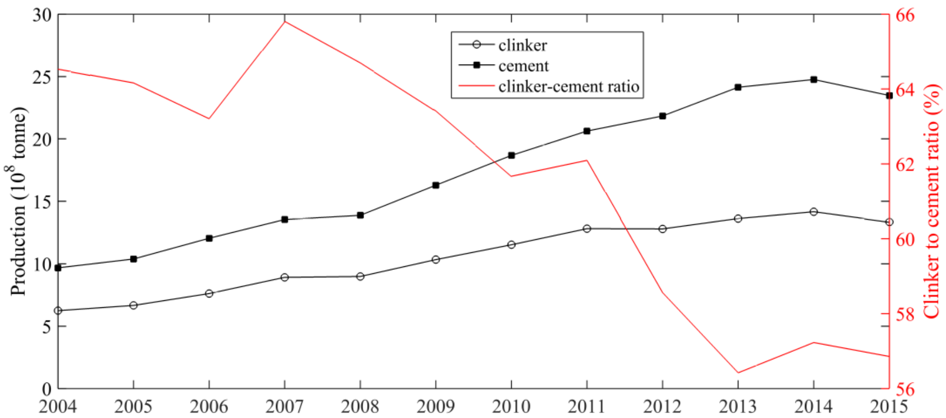

Figure S1. Annual productions of clinker and cement and their ratios in China.

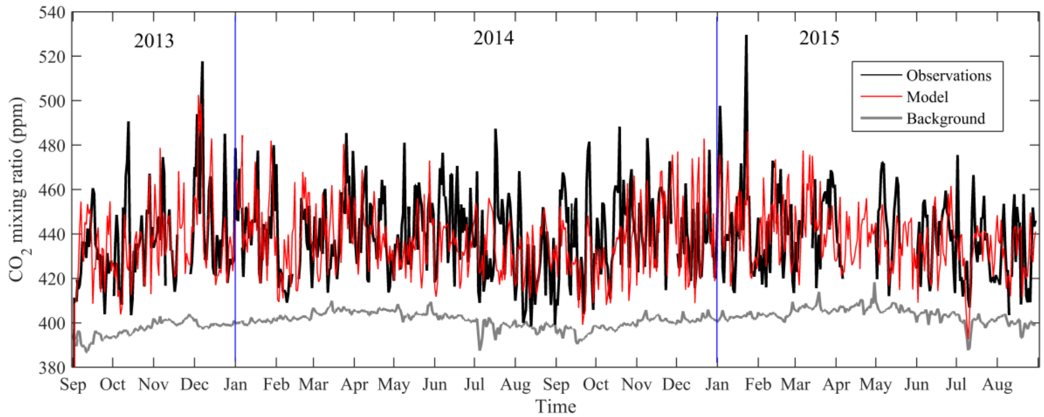

Figure S2. Daily comparisons of CO_2 mixing ratios.

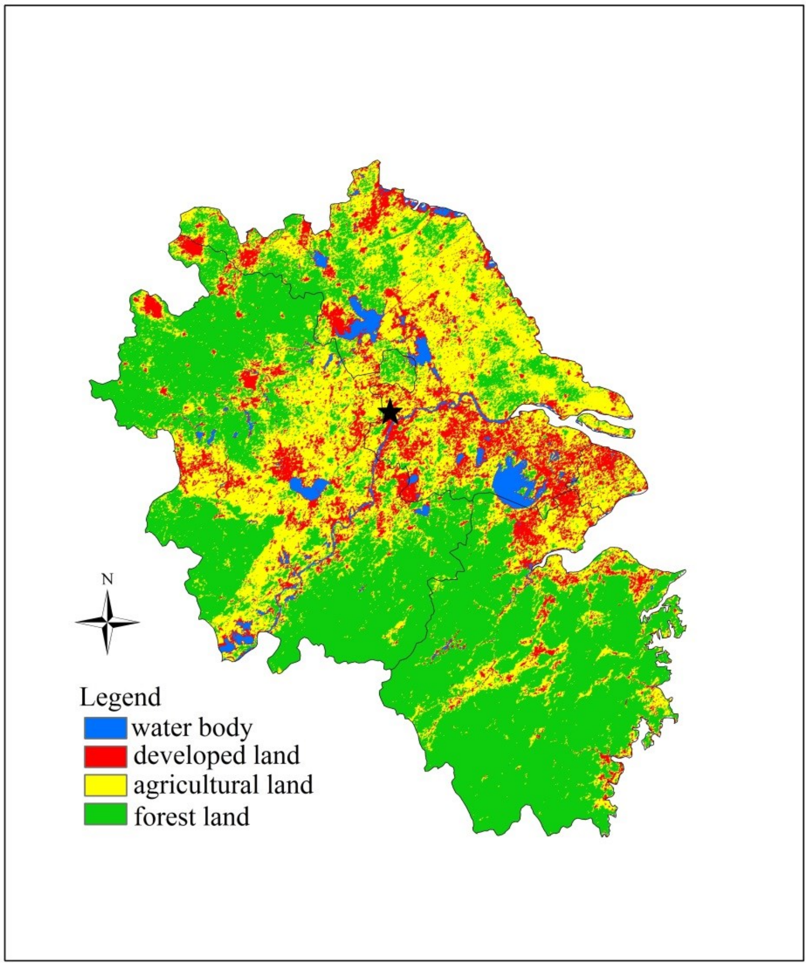

Figure S3. Land-Use and Land-Cover classification in Yangtze River Delta for 2014 was applied by using NDVI data of MOD13A2, '*' indicate observation site.

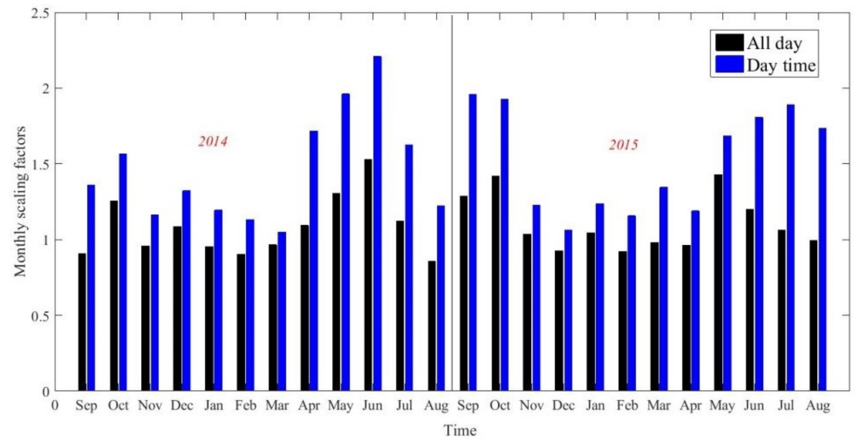

Figure S4. Derived monthly scaling factors for all-day and only daytime.

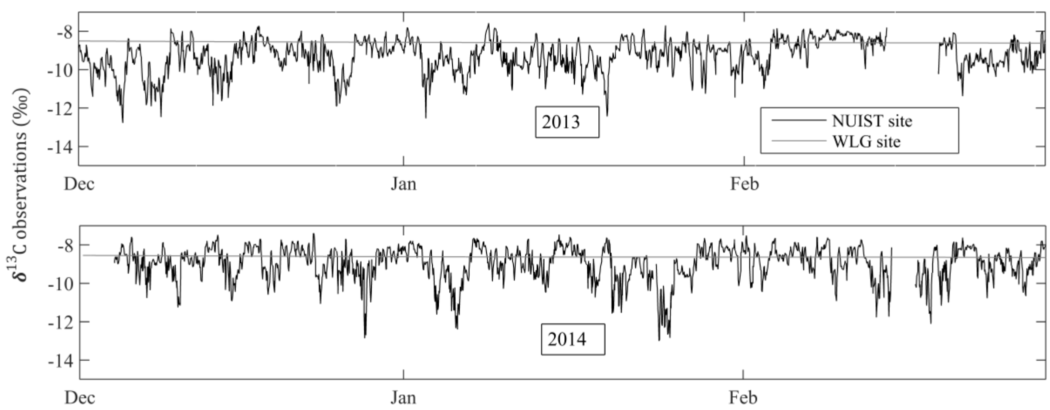

Figure S5. $\boldsymbol{\delta}^{13}$C Comparison between NUIST and WLG sites in winter.

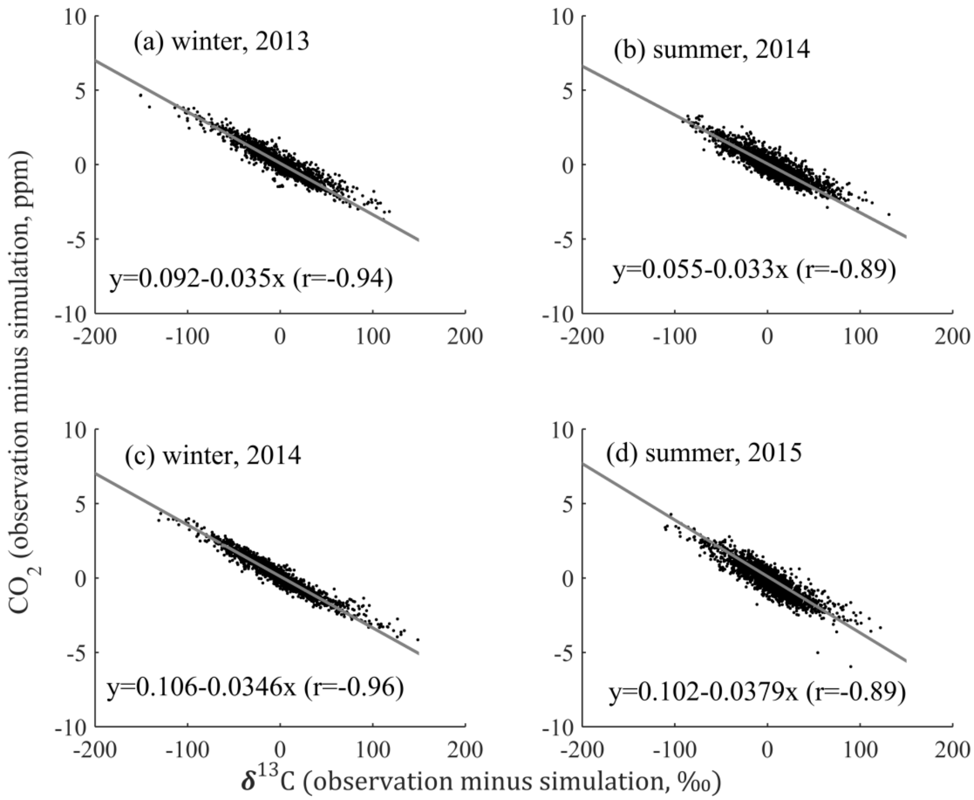

Figure S6. Relationship of observation minus simulation residual between CO_2 and $^{13}CO_2$ for (a) winter in 2013, (b) summer in 2014, (c) winter in 2014, and (d) summer in 2015.

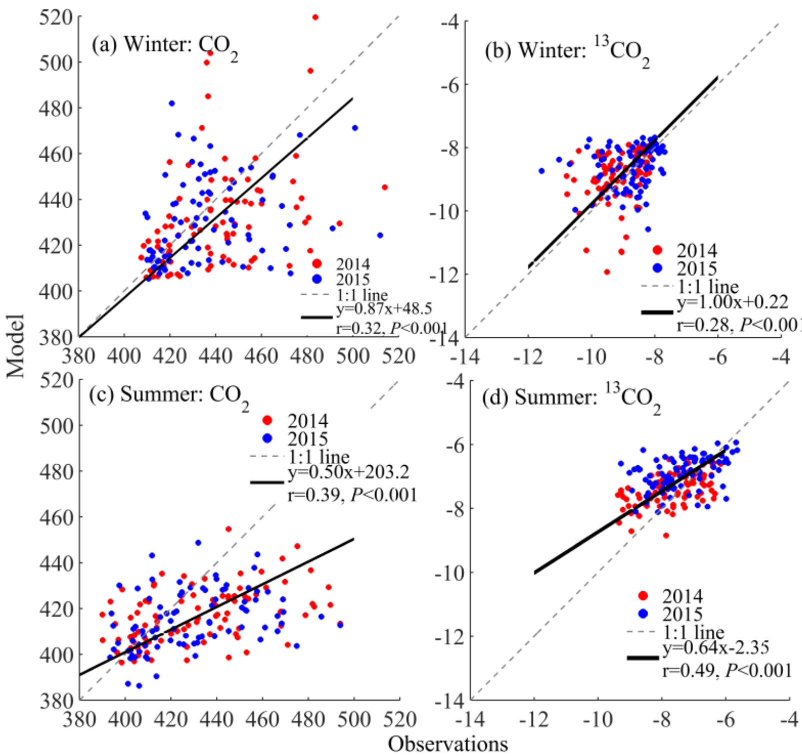

Figure S7. Scatter plots of observed versus modeled (a) winter time CO_2 mixing ratios, (b) winter time $\boldsymbol{\delta}^{13}C\text{-}CO_2$, (c) summer time CO_2, and (d) summer time $\boldsymbol{\delta}^{13}C\text{-}CO_2$ for both years, here these dots are daytime (10:00-16:00) averages.

Table S1. Difference of simulated monthly $\boldsymbol{\delta}^{13}C_{ms}$ between 2014 and 2015 for only anthropogenic sources.

	Jan	Feb	Mar	Apr	May	Jun	Jul	Aug	Sep	Oct	Nov	Dec
Nighttime (‰)	0.39	-0.16	-0.12	0.43	-0.25	1.06	0.75	0.56	-0.99	-1.09	0.00	-0.31
All-day (‰)	0.23	-0.14	-0.17	0.35	-0.25	0.32	0.67	0.20	-0.94	-0.95	-0.07	-0.22

Table S2. Comparisons between cement emission proportions and the simulated cement CO_2 enhancements proportions for different months in 2014 and 2015(note the superscript 'a' is ratio of cement to anthropogenic CO_2 emissions and 'b' is a ratio of cement to total CO_2 emissions, which contains biological and anthropogenic CO_2 flux).

Proportions	Jan	Feb	Mar	Apr	May	Jun	Jul	Aug	Sep	Oct	Nov	Dec	Annual ave
EDGAR anthropogenic ($\times 10^3$ $nmol \cdot m^{-2} \cdot s^{-1}$)	4.56	4.85	4.13	4.01	3.54	3.39	3.15	3.37	3.77	3.90	4.32	4.41	3.95
EDGAR cement ($\times 10^3$ $nmol \cdot m^{-2} \cdot s^{-1}$)	0.28	0.31	0.28	0.29	0.28	0.29	0.28	0.28	0.29	0.28	0.29	0.28	0.29
Cement emission proportion (%)	6.21	6.46	6.85	7.29	7.99	8.61	8.98	8.38	7.76	7.26	6.77	6.41	7.34
[a]Cement concentration proportion 2014 (%)	8.01	6.78	9.25	12.25	13.07	16.85	14.40	13.37	8.88	6.17	6.68	5.60	10.11
[a]Cement concentration proportion 2015 (%)	6.59	8.10	9.19	10.86	13.68	13.16	11.30	11.23	11.79	9.76	6.92	6.77	9.95
[b]Cement concentration proportion 2014 (%)	7.59	6.71	8.72	9.77	10.20	12.87	10.32	11.07	6.85	5.40	6.57	5.31	9.95
[b]Cement concentration proportion 2015 (%)	6.48	7.66	8.39	9.95	13.68	12.22	10.66	8.49	9.80	8.59	6.76	6.72	9.95